JACS
JOURNAL OF THE AMERICAN CHEMICAL SOCIETY

pubs.acs.org/JACS

Article

Rotaxanating Metallo-supramolecular Nano-cylinder Helicates to Switch DNA Junction Binding

Catherine A. J. Hooper,[●] Lucia Cardo,[●] James S. Craig, Lazaros Melidis, Aditya Garai, Ross T. Egan, Viktoriia Sadovnikova, Florian Burkert, Louise Male, Nikolas J. Hodges, Douglas F. Browning, Roselyne Rosas, Fengbo Liu, Fillipe V. Rocha, Mauro A. Lima, Simin Liu,* David Bardelang,* and Michael J. Hannon*

Cite This: *J. Am. Chem. Soc.* 2020, 142, 20651−20660

Read Online

ACCESS | Metrics & More | Article Recommendations | Supporting Information

ABSTRACT: A class of rotaxane is created, not by encapsulating a conventional linear thread, but rather by wrapping a large cucurbit[10]uril macrocycle about a three-dimensional, cylindrical, nanosized, self-assembled supramolecular helicate as the axle. The resulting pseudo-rotaxane is readily converted into a proper interlocked rotaxane by adding branch points to the helicate strands that form the surface of the cylinder (like branches and roots on a tree trunk). The supramolecular cylinder that forms the axle is itself a member of a unique and remarkable class of helicate metallo-drugs that bind Y-shaped DNA junction structures and induce cell death. While pseudo-rotaxanation does not modify the DNA-binding properties, proper, mechanically-interlocked rotaxanation transforms the DNA-binding and biological activity of the cylinder. The ability of the cylinder to de-thread from the rotaxane (and thus to bind DNA junction structures) is controlled by the extent of branching: fully-branched cylinders are locked inside the cucurbit[10]uril macrocycle, while cylinders with incomplete branch points can de-thread from the rotaxane in response to competitor guests. The number of branch points can thus afford kinetic control over the drug de-threading and release.

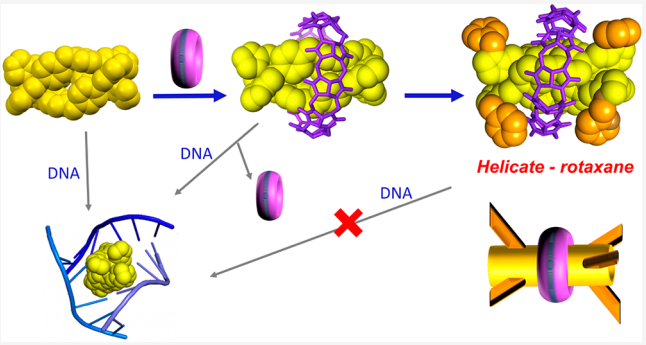

INTRODUCTION

Drawing on nature for inspiration, supramolecular chemistry has created a variety of complex, often exotic, nanoscale structures. Mechanically linked molecules have been of particular interest, and rotaxanes have been formed by threading molecular strands through a variety of different classes of macrocycle.[1−3] Applications of rotaxanes have ranged from protecting peptides from rapid enzymatic degradation, to creating materials with switchable surface properties.[1−8] Yet the threads used, to date, have been principally linear, 1-dimensional or 2-dimensional, organic, covalent molecules.

An alternative, but equally exciting, aspect of supramolecular chemistry, has been to take the designs and lessons of supramolecular chemistry and to apply them back to the biology that provided the initial inspiration for the field. Indeed self-assembled metallo-supramolecular helicates[9,10] are enjoying a resurgence of interest for their application in biology.[11−20] They offer quite large nanoscale surfaces of defined topography, of comparable scale to key structures found in biomolecules. We have used these external surfaces to access unique DNA- and RNA-recognition properties,[21−23] demonstrating with X-ray crystal structures the remarkable binding of cylindrical metallo-helicates in the heart of DNA and RNA 3-way junction structures,[24−28] where the nucleic acid bases form perfectly stacked aromatic interactions[29] with the external aromatic surfaces of the metallo-helicates. Nucleic acid junction structures are exciting targets found both in biology and nucleic acid nanoscience.[30−35] Our junction-binding cylinders arrest the proliferation of cancer cells and the HIV virus.[36−39]

Given that the supramolecular nano-cylinder helicates thread so beautifully *into and through* junctions and bulges in nucleic acids, we were intrigued to see whether we could push the boundaries of supramolecular assembly to similarly thread such self-assembled nanoscale metallo-supramolecular helicates through *synthetic* macrocycles to create new types of rotaxanes and pseudo-rotaxanes in which the thread was not a simple chain but a three dimensional, self-assembled, metallo-cylinder.

Received: July 18, 2020
Published: November 20, 2020

https://dx.doi.org/10.1021/jacs.0c07750
J. Am. Chem. Soc. 2020, 142, 20651−20660

Since the cylinders recognize DNA-junction structures through their external surfaces, we anticipated that wrapping another molecule around this region of the cylinder might also interfere with (and ultimately control) the DNA-binding. Rotaxanation in DNA-binding agents has not been previously explored.

We report now, for the first time, the wrapping of a synthetic macrocycle around the external surface of a self-assembled metallo-supramolecular nanostructure to create a pseudo-rotaxane, subsequent conversion to a proper (mechanically-interlocked) [2]-rotaxane, and the effect of rotaxanation on the biomolecular recognition and biological properties of the metallo-supramolecular cylinders. Examples of larger threads in rotaxanes include pseudo-rotaxanes created by clipping macrocycles around carbon nanotubes,[40,41] a rotaxane with a spherical fullerene in the center,[42] and DNA rotaxanes,[43] but this work is distinct in representing (to the best of our knowledge) the first example of a proper interlocked rotaxane assembled around a three-dimensional metal-assembled supramolecular helicate as axle. An interesting report of rotaxanation of a helical peptide has also appeared, but in that case the small rotaxane ring wraps just around its linear chain (primary structure) rather than encapsulating a helical secondary structure.[44] The large three-dimensional cylindrical surface that our metallo-supramolecular helicate axle affords also brings another opportunity: rather than attaching a branched organic unit at each end of the thread as a stopper, we now clip unbranched units onto each thread of the helicate axle exploiting the metal-coordination and supramolecular structure to achieve the branching effect which mechanically constrains the ring. We show that the rotaxanation allows us to switch the DNA-binding properties and thus the biological activity of the cylinder.

RESULTS AND DISCUSSION

The first challenge was to identify a suitable "ring" that might be wrapped around these metallo-supramolecular helicates. They are tetracations formed by wrapping three organic ligand strands about two metal centers (Figure 1).[11] They are cylindrical in shape, around 2 nm in length, and 1 nm in diameter—much greater than the dimensions normally associated with rotaxanation or encapsulation—but we identified that cucurbit[10]uril (Figure 1) might offer a cavity of suitable dimensions.[45,46]

Cucurbit[*n*]urils (CB[*n*]s) are a class of macrocycles that are attracting much attention for both host–guest chemistry and rotaxanation studies.[45−52] They are pumpkin-shaped molecules with a rigid hydrophobic cavity flanked by two identical openings (portals) whose rims are each lined with *n* carbonyl groups. CB[5,6,7] are ideal sizes for traditional small organics and CB[6,7,8] have been used with organic, linear threads and chains to create rotaxanes.[48] Other applications have included using the host guest chemistry to attach proteins to surfaces or fluorophores, and for drug delivery.[47,53] The largest of the class, with an untwisted cavity, is CB[10] (Fig. 1) which can accommodate multiple or larger molecules[45,46] as demonstrated by its use to capture both a Stoddart "blue-box" (bis-bipyridinium) macrocycle and its methoxybenzene guest to create a Russian-doll style assembly.[54] Binding interactions include hydrophobic effects in the heart of the cavity and ion-dipole interactions at the rims.[45−54]

While lower order cucurbiturils have relatively rigid cavities, CB[10] is more flexible. It is observed to be ellipsoidal in its crystal structure (cavity diameter 1.13-1.24 nm; portal

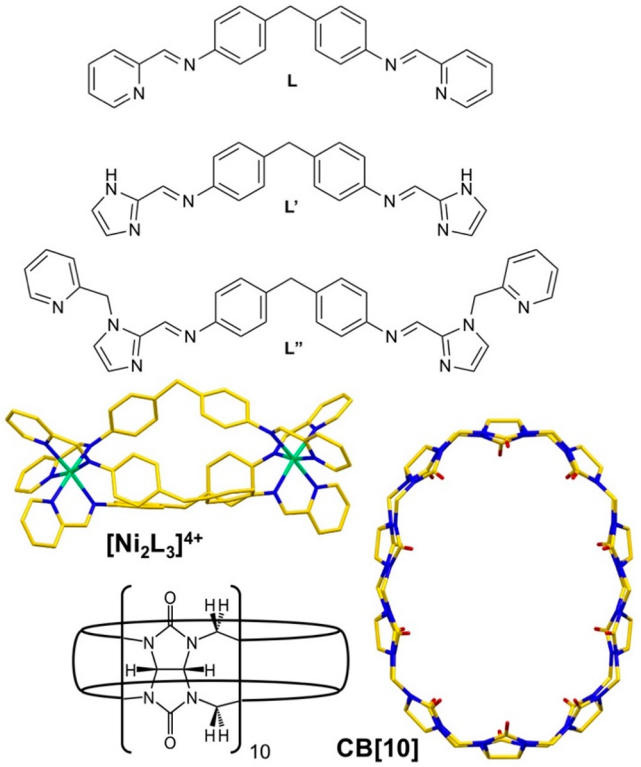

Figure 1. Ligands used in this study together with the structure of the $[Ni_2L_3]^{4+}$ cylinder (CSD-NITBIB) and cucurbit[10]uril (from CSD-LAZPIM and illustrating the flexibility and potential ellipsoidal distortions CB[10] can accommodate in response to guests).

diameter 0.95-1.06 nm) in complex with 4,6-bis(4-(ammoniomethyl)phenylamino)-1,3,5-triazen-2(1H)-one,[45,46] and it is observed to also complex platinum terpyridyls[55] and porphyrins[56] which implies further distortion is possible. The previous use of CB[10] for rotaxanation is restricted to a report of a kinetic rotaxane—a pseudo-rotaxane in which the thread is encapsulated at room temperature but can enter and leave at elevated temperatures.[57]

To initiate our studies we first explored whether the supramolecular cylinders would bind to CB[10] to give a tube threaded through a ring. CB[10] itself is an insoluble compound, but rapidly dissolves on addition of an aqueous solution of $[M_2L_3]^{4+}$ cylinders (M = Fe, Ru, Ni). Electrospray mass spectrometry shows peaks corresponding to $[M_2L_3{\cdot}CB10]^{4+}$ (Figure S1 of the Supporting Information, SI) and proton NMR spectroscopy of $[Fe_2L_3]^{4+}$ with CB[10] confirms formation of a 1:1 complex (Figure 2). DOSY NMR reveals that a single species is formed, of greater hydrodynamic radius than the free cylinder, and involving both cylinder and CB[10]. The cylinder retains its two-fold and three-fold symmetry in the complex. The proton NMR resonances corresponding to the central CH_2 of the cylinder and the adjacent phenylene protons experience upfield shifts, consistent with a shielded location in the CB[10] cavity, while the imine proton and the pyridine H_3 are shifted downfield, consistent with encountering the carbonyls at the rim of the macrocycle. NOEs are observed from these two cylinder protons (H_{im} and H_3) to the CH_2 proton on the rim of the CB[10] macrocycle (Figure S2). The NMR is unambiguous confirmation that the cylinder sits symmetrically (on the NMR time scale) in the center of the macrocycle threading through from one side to the other as a

https://dx.doi.org/10.1021/jacs.0c07750
J. Am. Chem. Soc. 2020, 142, 20651−20660

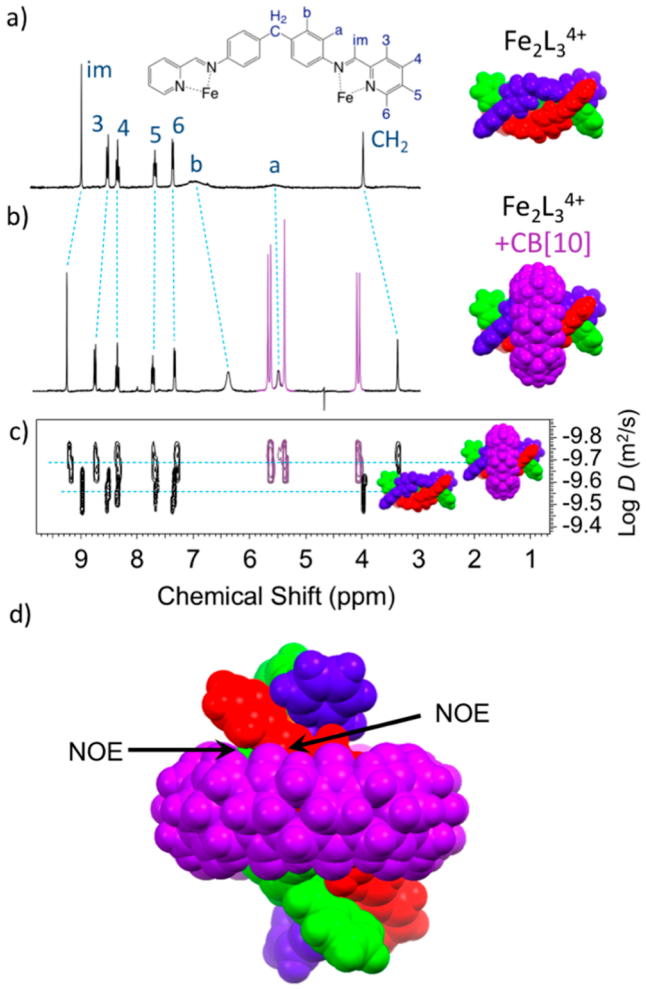

Figure 2. 500 MHz ^{1}H NMR spectra of the $[Fe_2L_3]^{4+}$ cylinder (0.5 mM) (a) alone and (b) with 1 equiv of CB[10] in D_2O illustrating the shifts caused by binding. (c) DOSY NMR spectra (stacked) showing the change in diffusion coefficient on binding consistent with formation of a single species of increased hydrodynamic radius. (d) DFT model of the cylinder + CB[10] also showing the experimentally observed NOEs from cylinder H-im & H-3 to a CH_2 proton on the rim of the CB[10].

pseudo-rotaxane, with the macrocycle sitting over the central diphenylmethanes of the cylinder as desired. To retain its three-fold symmetry within the 10-fold symmetric CB[10], the cylinder must be rapidly spinning or rocking about the metal−metal axis while within the macrocycle. DFT calculations and MD simulations reproduce this solution structure, with the DFT structure showing axial deviation between the host and guest main symmetry axes at the energy minimum (Figure 2d) and the MD showing the rotation. The binding of the cylinder places the diphenylmethane units within the hydrophobic cavity and does not leave space for solvent to co-bind in the cavity—water exclusion is understood to be an important part of CB[*n*] guest binding.[45−54] The positively-polarized imino and pyridyl CH protons are located close to the oxygen-rich rim (as indicated by the NOEs to the CH_2 at the rim) though individual CH···O interactions must be transient since the cylinder is rotating rapidly. Use of a small excess of cylinder (Figure S3) in the NMR allows free and bound cylinder peaks to be observed indicating that exchange is slow on the NMR time scale, however on mixing $[Fe_2L_3]^{4+}$ with $[Ni_2L_3{\cdot}CB10]^{4+}$ and immediately injecting into an electrospray mass spectrometer a mixture of $[Fe_2L_3{\cdot}CB10]^{4+}$ and $[Ni_2L_3{\cdot}CB10]^{4+}$ was observed, the ratio of which remained unchanged over a further hour of sampling (Figure S4). Together these observations indicate that the exchange takes place over a time scale of milliseconds to seconds, which is consistent with measurements on other cucurbiturils with different guests.[58] The proton NMR spectrum of $[Ru_2L_3]^{4+}$ with CB[10] shows analogous upfield and downfield shifts in the resonances and the paramagnetically shifted proton NMR of $[Ni_2L_3]^{4+}$ with CB[10] also shows the binding (Figures S5 and S6).

While the ruthenium(II) and nickel(II) $[M_2L_3]^{4+}$ cylinders have excellent stability, the iron(II) cylinders can experience some hydrolytic degradation over long periods,[11,37] although they are stabilized by binding to DNA.[21,22] Encapsulation of the cylinder within the CB[10] macrocycle similarly enhances the cylinder stability; an experiment with 0.9 equiv of CB[10] revealed no degradation of the bound cylinder in aqueous solution over a period of 194 days (Figure S7). The insolubility of unbound CB[10] prevents accurate measurements of binding affinity with guests, however an NMR dilution experiment showed no unbound cylinder (Figure S8) implying the binding constant is greater than 10^7 M^{-1}, and NMR competition studies show that the cylinder binds more strongly than both methyl viologen and memantine hydrochloride.

To explore the effect of the encapsulation on the cylinder's DNA-recognition properties we investigated the binding of the nickel cylinder·CB[10] complex (as representative of the three complexes) to DNA 3-way junctions (3WJ)[24−28,30,31] using gel electrophoresis. The assay (Figure 3a) uses a 3WJ formed from three different complementary DNA strands. The 3WJ structure is (entropically) unstable at room temperature in absence of the cylinder, and the DNA exists as three single strands. When the cylinder binds, the 3WJ is stabilized and observed in the gel. Radiolabelling one strand allows a simple on/off gel-shift binding assay that is readily visualized. Figure 3a shows that the cylinder·CB[10] complex stabilizes the 3WJ and the effect of the cylinder·CB[10] complex is the same as the cylinder alone, although higher loadings are required. This indicates that the cylinder can leave the CB[10] cavity and bind to the anionic DNA 3WJ cavity; while binding of an intact cylinder·CB[10] complex to the 3WJ cannot be excluded this would be expected to give a different gel shift. The cylinder binding to the 3WJ is in competition with the binding to the CB[10]; adding small amounts of solid CB[10] or of the soluble methylviologen CB[10] complex to the pseudorotaxane leads to small reductions in 3WJ formation (Figure S9). In these experiments, the binding energy to the 3WJ also incorporates the energetic cost of assembling the 3WJ from the DNA single strands. Given that the 3WJ is not observed in absence of cylinder at room temperature, the binding constant of cylinder to the 3WJ structure itself must be (significantly) greater than that to CB[10].

We also studied the binding to calf-thymus DNA (a polymeric genomic DNA), using circular and flow linear dichroism spectroscopies (Figure 3b,c). The effects are again the same as the free cylinder binding: The circular dichroism confirms binding of cylinder (an induced CD signal is observed in the cylinder spectroscopy between 300-400 nm) and retention of a B-DNA structure (typical signature between 200-300 nm). The CD spectra are the same as those observed with cylinder alone (Figure S10), although at high loading some scattering is observed consistent with release of CB[10]

https://dx.doi.org/10.1021/jacs.0c07750
J. Am. Chem. Soc. 2020, 142, 20651−20660

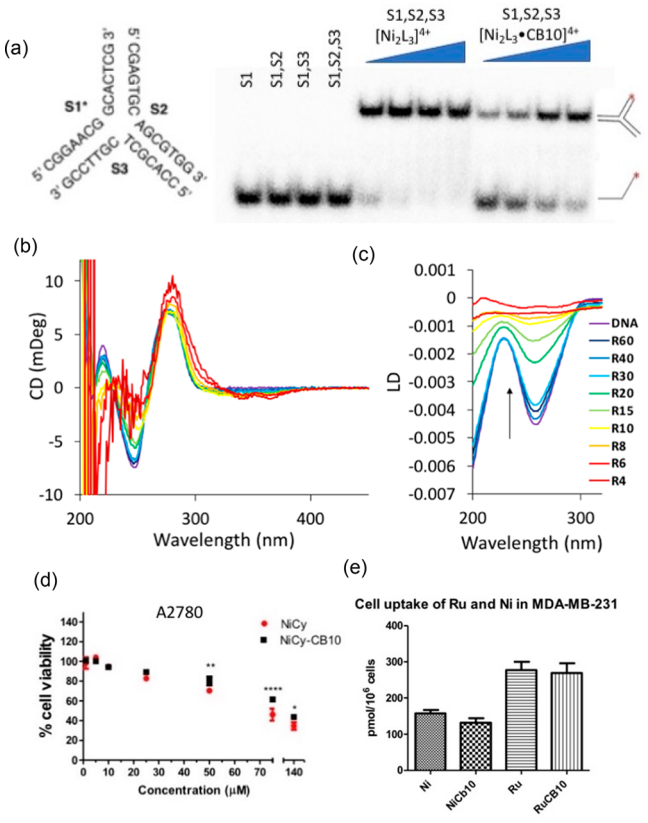

Figure 3. (a) PAGE gel showing that the $[Ni_2L_3{\cdot}CB10]^{4+}$ complex stabilizes DNA 3WJ in the same way as $[M_2L_3]^{4+}$ cylinders alone. (* = radiolabel) (b) CD and (c) LD spectra of ct-DNA (100μM DNA concentration; 10 mM sodium chloride; 1 mM sodium cacodylate) with $[Ni_2L_3{\cdot}CB10]^{4+}$. *R* values represent DNA base pairs/complex. The spectra show binding and DNA coiling and importantly are analogous to those obtained with free $[Ni_2L_3]^{4+}$ (Figure S10) (d) MTT cell survival assay (72 h treatment of A2780 cells), demonstrating that $[Ni_2L_3{\cdot}CB10]^{4+}$ and $[Ni_2L_3]^{4+}$ have similar effects on cell survival (triplicate independent repeats; ±SD; two way ANOVA analyses). (e) Cell uptake studies (triplicate; ±SD) demonstrating that CB[10] does not affect the cell uptake. The greater uptake of the Ru (over Ni) cylinder is consistent with previous observations in 1G5 (Jurkat T-) cells.[37]

which (uncomplexed) will be insoluble. The flow linear dichroism experiments probe the orientation of ct-DNA in a Couette flow cell, with the magnitude of the peak at 260 nm reflecting the orientation.[21,22] Cylinders are known to coil ct-DNA (leading to a loss of orientation);[21,22] the spectra on addition of the cylinder·CB[10] complex confirm the same DNA-coiling effects and are analogous to those observed with free cylinder (Figure S10). We conclude that while the CB[10] does bind the cylinder in solution to form the pseudo-rotaxane, the cylinder would prefer to bind to anionic DNA. For the 3WJ, which is not pre-formed in solution, the extra energy of forming the structure means that there is competition between binding CB[10] or 3WJ. When presented with a polymeric DNA anion, the cylinder leaves the CB[10] cavity and binds its preferred partner. Preferential binding to the anionic DNA over the neutral CB[10] cavity is unsurprising, given the anticipated electrostatic contribution to that binding energy, though it contrasts with spermine that preferentially binds CB[7] over DNA.[59]

Consistent with the in vitro DNA binding, when we treat cells (A2780 ovarian and MDA-MB-231 breast cancer lines) with the cylinder·CB[10] complex, we observe very similar inhibitions of cell proliferation (as assessed by an MTT assay) to those with the corresponding free cylinder (Figures 3d and S11). There is a very slight enhancement in activity for the ruthenium cylinder but a slight drop in activity for the iron and nickel cylinders. Uptake studies (assessed by ICP−MS) indicate that the encapsulation inside CB[10] has little effect on the extent of overall uptake (Figure 3e). Cucurbiturils are frequently used as drug delivery agents and platinum metallodrugs (e.g., oxaliplatin) encapsulated inside cucurbit[7]uril show some enhanced effects[60−65] due to better uptake and/or pharmacology (less degradation and side reactions with thiols). The lack of dramatic enhancement for the cylinder perhaps reflects the already excellent cell uptake of cylinders[36,37] and the lack of competing side reactions. The DNA-binding studies indicate that whether the cylinders have entered alone or in complex with CB[10], their effects when they reach the target DNA are expected to be the same. Consistent with this, a dinuclear ruthenium complex (from Keene, Collins et al.)[66,67] that also binds non-covalently to DNA, and that can partially

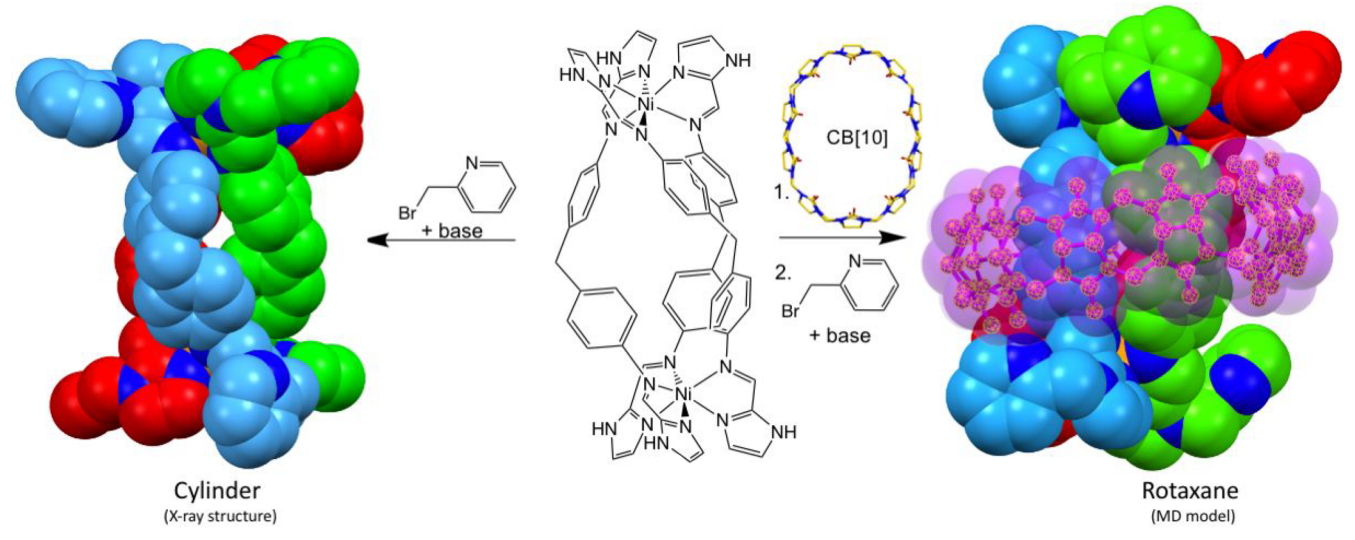

Figure 4. Our synthetic strategy to create a rotaxanated cylinder.

https://dx.doi.org/10.1021/jacs.0c07750
J. Am. Chem. Soc. 2020, 142, 20651−20660

insert (but is too large to thread) into CB[10], similarly showed only small effects of complexation on its in cellulo behavior (though the DNA-binding of that agent is different and the complex only mildly cytotoxic).

Having established that pseudo-rotaxanation with CB[10] was readily achieved and that it placed the macrocycle in the correct position over the central section of the cylinder but that it had little effect on the biological properties due to competitive de-threading, we next explored if we could lock the macrocycle onto the cylinder as a proper rotaxane. Traditional rotaxanes are formed by attaching two bulky stoppers, one at each end of the thread. By using a 3-dimensional helicate as the axle, we open up an alternative possibility to create the branching needed to lock the ring onto the structure, by attaching multiple (smaller) groups that protrude out of the cylindrical surface at the ends of the helicate axle. To explore this, we modified the design of the cylinder, replacing the pyridines with 2-imidazole units. The 2-imidazole offers a position to which we can add further functionalization, through alkylation of the non-coordinated nitrogen in the imidazole ring, and we selected 2-picolyl as the alkylating group. Thus, we introduce three branch points onto the cylinder surface at each end. This new design approach is shown in Figure 4.

We first prepared two non-rotaxanated cylinders, $[Ni_2L'_3]^{4+}$ and $[Ni_2L''_3]^{4+}$, analogous to the parent cylinders but bearing the 2-imidazole and 2-imidazole-*N*-picolyl groups in place of the pyridines. They are readily prepared from the condensation of the 2-imidazole and 2-imidazole-*N*-picolyl carboxaldehdyes with bis-1,4-diaminophenylmethane and subsequent coordination to nickel(II). While the corresponding iron(II) complexes were also prepared, $[Fe_2L'_3]^{4+}$ had a lower solution stability than the corresponding nickel(II) complex and so we focused our studies on the nickel complexes. The X-ray crystal structures of the $[M_2L''_3]^{4+}$ cations (M = Ni, Fe) were obtained (as the hexafluorophosphate salts) and confirmed the expected structure (Figures 4 and S12), with the retention of the triple-helical cylindrical structure, the retention of the central core of the cylinder structure which is crucial for its binding to both DNA 3-way junctions and CB[10], and now the introduction of the picolyl units sticking out of the helix and in such a position that they should not interfere with the CB[10] binding site but would potentially sterically prevent it from threading/dethreading.

We then explored whether we could post-synthetically transform $[Ni_2L'_3]^{4+}$ into the alkylated $[Ni_2L''_3]^{4+}$ by reaction with alkylating agent 2-(bromomethyl)pyridine and Hunig's base in acetonitrile; heating at reflux overnight afforded the desired hexa-alkylated product, $[Ni_2L''_3]^{4+}$, as confirmed by mass spectrometry and (paramagnetic) proton NMR spectroscopy. Small amounts of the penta-functionalized cylinder were also observed by mass spectrometry. To access the rotaxane, we then repeated the same reaction in the presence of CB[10]. While acetonitrile did not prove to be a suitable solvent, reaction in aqueous methanol at reflux overnight, afforded the rotaxane as a cream precipitate in ~60% isolated yield. The mass spectrum (Figures 5 and S14) shows a dominant peak corresponding to $[Ni_2L''_3{\cdot}CB10]^{4+}$ (correct mass and isotope distribution). Smaller peaks corresponding to penta-alkylated rotaxanes are also observed but only a tiny trace peak corresponding to un-rotaxanated $[Ni_2L''_3]^{4+}$ indicating that the rotaxane (as opposed to a pseudo-rotaxane)

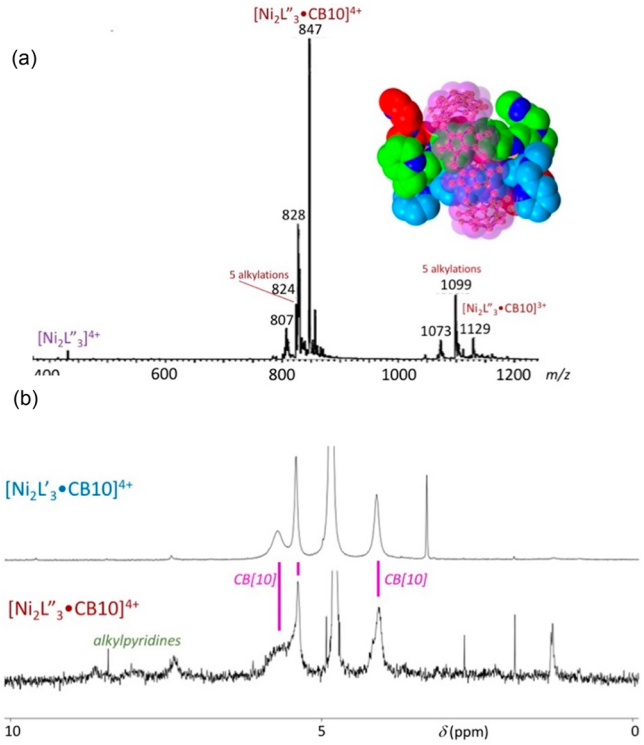

Figure 5. (a) Mass Spectrum of the $[Ni_2L''_3{\cdot}CB10]^{4+}$ rotaxane (b) ^{1}H NMR Spectrum (0−10 ppm shown only) of the $[Ni_2L''_3{\cdot}CB10]^{4+}$ rotaxane and comparison with imidazole pseudo-rotaxane $[Ni_2L'_3{\cdot}CB10]^{4+}$ showing presence of CB[10] and the alkylpyridine groups on the modified cylinder.

is formed in which the ring is now constrained by the picolyl groups to remain on the cylinder.

The (paramagnetically shifted) proton NMR spectrum shows the presence of peaks corresponding to the cylinder and the CB[10] (Figures 5 and S13). The cylinder peaks in the rotaxane are further broadened than those observed in the free $[Ni_2L''_3]^{4+}$ cylinder; consistent with this, MD simulations (Figures 4 and 6) indicate that the picolyl groups restrict the spinning motion of the cylinder about the metal−metal axis while rotaxanated inside the CB[10]. The rotaxanated complex $[Ni_2L''_3{\cdot}CB10]^{4+}$ was mixed with an equimolar amount of $[Fe_2L_3]^{4+}$ and heated under reflux for 24 h in 10% methanol/water. The rotaxane was unchanged and no Fe_2L_3 pseudo-rotaxanes were observed by mass spectrometry; this contrasts with the analogous mixing experiments with pseudo-rotaxanes and is strong evidence of proper rotaxane formation.

Rotaxanation would also be expected to enhance the inherent stability of the cylinder and to explore this we treated the picolyl functionalized cylinder $[Ni_2L''_3]^{4+}$ and the rotaxane $[Ni_2L''_3{\cdot}CB10]^{4+}$ with EDTA. EDTA binds strongly to Ni^{2+} in water ($\log K > 18$)[68] and is able to remove nickel from $[Ni_2L''_3]^{4+}$ over a period of hours at room temperature. The rotaxanation does provides additional stabilization, and the rotaxanated cylinder is competitive with EDTA for nickel binding (Figure S21) with significant amounts of rotaxane still present even after treatment with 10 equiv of Na_2(EDTA).

Multiply-threaded rotaxanes are structures of considerable interest.[69−71] Considering only the ligands of the helicate the rotaxane might be viewed as a [4]rotaxane with two metal bound to the three strands. However, mass spectrometric analysis demonstrates that on demetallation the ligands are no

https://dx.doi.org/10.1021/jacs.0c07750
J. Am. Chem. Soc. 2020, 142, 20651−20660

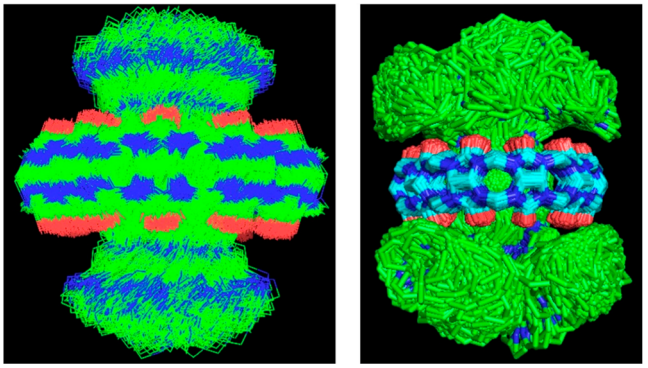

Figure 6. Combined and superimposed views of Molecular Dynamics simulations of the pseudo-rotaxanated $[Ni_2L'_3{\cdot}CB10]^{4+}$ (left) and proper rotaxanated $[Ni_2L''_3{\cdot}CB10]^{4+}$ (right) complexes showing the free rotation of the $[Ni_2L'_3]^{4+}$ cation in the CB[10] and the more restricted motion caused by the picolyl groups for $[Ni_2L''_3]^{4+}$; in the 1 μs time scale the rotaxanated cylinder does not rotate. Hydrogens are omitted for clarity. Supplementary videos of the simulations are also available. There is a tendency for the CB[10] ring to undergo fluxional distortions during the simulation, including a buckling of the ring at the CH_2 groups that create a heart-shaped ring and allowing it to close up around the cylinder. This is also seen at very low frequency (<0.1%) in simulations of the free CB[10] but is more prevalent in the rotaxane. The paramagnetic broadening in the ^{1}H NMR does not allow this feature to be confirmed experimentally but reflects the greater flexibility of CB[10] compared to lower order cucubit[*n*]urils. See also Figures S18 and S25.

longer sterically constrained in the CB[10] cavity and dethread (Figure S21). The metallo-supramolecular assembly of the triple-helicate is thus crucial to the design and rotaxane preparation, and we consider a [2]rotaxane nomenclature to be more appropriate for this particular supramolecule, though it might be possible to access [4]rotaxanes by this approach in the future using bulkier groups.

The *non-rotaxanated* $[Ni_2L'_3]^{4+}$ and $[Ni_2L''_3]^{4+}$ cylinders bind DNA analogously to the original pyridyl cylinders (Figures 7, S16, and S17). PAGE gel electrophoresis experiments confirm that both are able to bind and stabilize DNA 3-way junctions, just as the original pyridyl cylinders do, with $[Ni_2L'_3]^{4+}$ less effective than the parent (perhaps due to imidazole deprotonation) and $[Ni_2L''_3]^{4+}$ slightly more so (perhaps because of its larger surfaces which extend into the 3WJ grooves—Figure S22). Circular dichroism spectra confirm that both cylinders bind calf thymus DNA (inducing a CD signal in the cylinder spectroscopy) which retains a B-DNA structure, and the linear dichroism demonstrates that both cylinders give rise to DNA-coiling as observed with pyridyl-based cylinders. Cell proliferation (MTT) assays confirmed that the functionalized (but non-rotaxanated) cylinder $[Ni_2L''_3]^{4+}$ exerts a cytotoxic effect in cells (IC_{50}, 72 h, MDA-MB-231 55 ± 10 μM; SKOV3 52 ± 5 μM). Thus, as anticipated, making changes to the ends of these cylinders does not, of itself, prevent the key DNA-binding and biological activities.

The contrast with the *rotaxane* $[Ni_2L''_3{\cdot}CB10]^{4+}$ is striking (Figure 7). The rotaxane can no longer stabilize the DNA 3WJ in the gel electrophoresis experiment. It also no longer coils DNA (rather a small increase in DNA orientation is observed). Thus, wrapping the CB[10] macrocycle around the central phenylene units has switched off the DNA junction binding and DNA coiling as anticipated. The greater DNA orientation

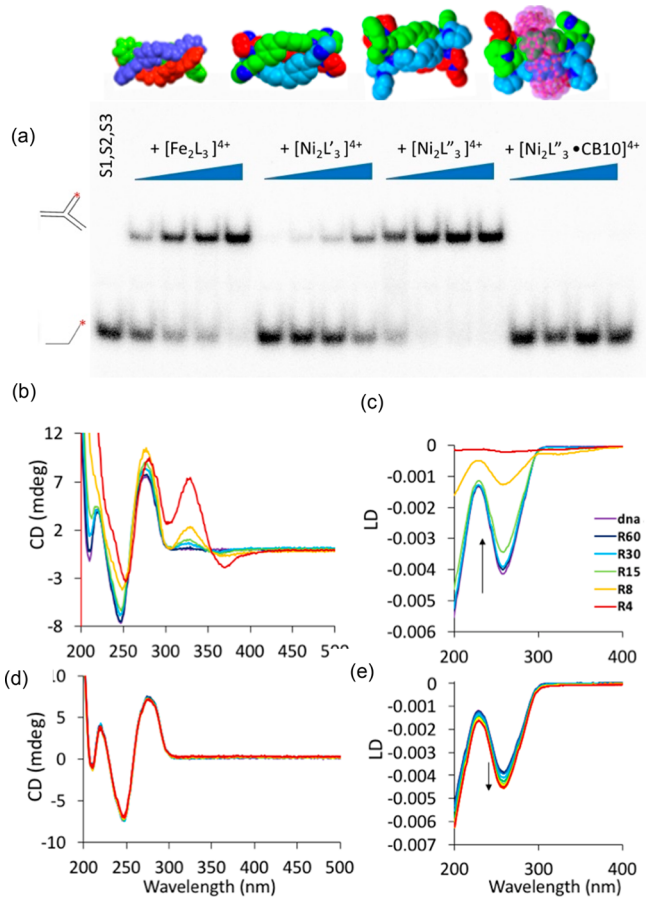

Figure 7. (a) PAGE gel showing that the $[Ni_2L'_3]^{4+}$ and $[Ni_2L''_3]^{4+}$ complexes stabilize DNA 3WJ but the rotaxanated $[Ni_2L''_3{\cdot}CB10]^{4+}$ cylinder does not. (b) CD and (c) LD spectra of ct-DNA (100μM DNA concentration; 10 mM sodium chloride; 1 mM sodium cacodylate) with $[Ni_2L''_3]^{4+}$ and (d) the corresponding CD and (e) LD spectra of ct-DNA with $[Ni_2L''_3{\cdot}CB10]^{4+}$. *R* values represent DNA base pairs/complex.

observed in a Couette cell in the linear dichroism experiment indicates some form of DNA binding occurs, while the circular dichroism confirms that the DNA remains in its B form. Molecular dynamics simulations (Figure S18) suggest that the rotaxane may associate through a partial entry into the grooves, and that this leads to some small elongation of the DNA. Association with the bases at the ends of the DNA strand is also seen in the simulations together with some capacity to bridge across two pieces of DNA that could also lead to enhanced orientation in a Couette cell.

Just as the rotaxanation switches off the key DNA binding features of the cylinders, it also switches off the biological action with the rotaxane showing no cytotoxic effect in cell proliferation (MTT) assays (IC_{50}, 72 h ≫140 μM) in MDA-MB-231 (breast) cell lines (Figure S11).

To explore thread release we prepared a rotaxane mixture in which we only partially alkylated the rotaxane, thereby varying the number of picolyl branches/stoppers on the species, and creating a mixture of rotaxanes containing 3-, 4-, and 5-stoppers on the thread as well as the fully-stoppered 6-alkylated rotaxane (Figure 8). We then undertook a competition experiment with the $[Fe_2L_3]^{4+}$ cylinder (Figures 8 and S23).

The results are consistent with a kinetic de-rotaxanation for cylinders that are not fully stoppered: the competitor initially

https://dx.doi.org/10.1021/jacs.0c07750
J. Am. Chem. Soc. 2020, 142, 20651−20660

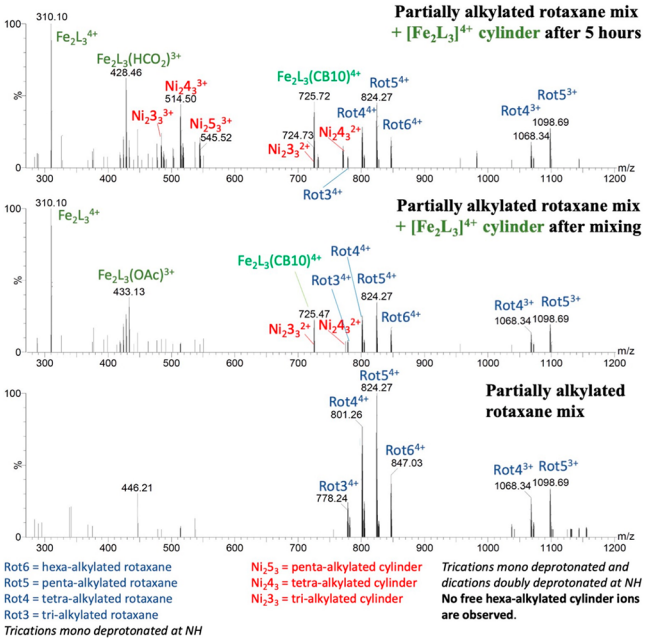

Figure 8. Electrospray mass spectra of a competition experiment treating a partially alkylated rotaxanate mix $[Ni_2L''_3{\cdot}CB10]^{4+}$ with 1 equiv of $[Fe_2L_3]^{4+}$ in aqueous methanol (1:1) showing the dethreading of partially alkylated cylinders and the formation of pseudo-rotaxane $[Fe_2L_3{\cdot}CB10]^{4+}$. No peaks corresponding to dethreading of fully alkylated (hexa-alkylated) cylinders were observed. Figure S23 shows further timepoints.

displaces tri- and tetra-alkylated cylinders from the CB[10] ring and after further time also penta-alkylated cylinders. No peaks corresponding to displacement of hexa-alkylated (fully alkylated) cylinders are observed even over long time periods (28 h). An analogous experiment with 5 and 10 equiv of competitor guest memantine (Figure S24a) showed similar effects.

The tri-alkylated cylinders, at one end bear just one or no stoppers, and the tetra-alkylated cylinders have an end with either one or two stoppers. The penta-alkylated cylinder has one end with two stoppers, while in the hexa-alkylated cylinder both ends contain three stoppers. The results imply that cylinders with a mono-alkylated end de-thread more readily than those whose ends are di-alkylated, consistent with the greater steric barrier to de-threading that increased alkylation should present.

This poorly alkylated rotaxane mixture also gave rise to a weak 3WJ band in gel electrophoresis (Figure S24b), consistent with a small proportion of poorly alkylated cylinders dethreading from the CB[10] and binding instead to the 3WJ. These results provide intriguing insight into how the extent and type of branch-point alkylation might be used to control the kinetics of de-rotaxanation and in turn kinetically and temporally modulate release of the 3WJ-binding drug.

CONCLUSIONS

We have demonstrated a new approach to the design of rotaxanes by employing cylindrical metallo-supramolecular helicates as the axle, with the ring held in place by branch points which emanate from the strands of the helix. These intriguing new agents are assembled by combining two designs on which the field of supramolecular chemistry was founded: the metallo-helicates (pioneered by Lehn)[9] and rotaxanes (Stoddart and Sauvage).[1,2] The metallo-cylinders (a class of triple-helicates) used as the rotaxane axle, offer unique and unprecedented DNA binding properties; their activity has stimulated a great interest in designing metallo-supramolecular drugs.[11,12] Pseudo-rotaxanation is not sufficient to modify the bio-activity of these cylinders in vitro or in cellulo, but by proper rotaxanation those properties are modified.

Switching the activity of a *metallo*-drug on rotaxanation represents an unconventional approach: indeed incorporation of metallo-drugs into *proper* rotaxanes is rare and restricted to mononuclear platinum[72] and ruthenium[73] drugs attached to the terminal stopper of a rotaxane, with the rotaxane part essentially behaving as an attached organic vector. Organic drugs such as paclitaxel have also been attached as a rotaxane stopper,[74] while Papot and Leigh have used a potentially bioactive peptide as a linear thread in a hydrogen-bond assembled rotaxane and combined it with a sophisticated enzyme-cleavage rotaxane degradative release.[75,76]

Beyond the temporal control of activity that we explore, our results also raise the tantalizing possibility of creating systems in which a triggered rotaxanation or de-rotaxanation (de-threading) inside a cell might be used to switch a metallo-drug action on or off. This might be applicable to a range of different molecular and metallo-supramolecular designs and we are actively exploring the further potential of this approach.

ASSOCIATED CONTENT

Supporting Information

The Supporting Information is available free of charge at https://pubs.acs.org/doi/10.1021/jacs.0c07750.

Experimental details and Figures S1−S25 (PDF)
Movie of the MD simulations in Figure 6 (MP4)
Movie of the MD simulations in Figure 6 (MP4)
Crystallographic file for $[Ni_2L_3'']$[PF_6]$_4$ (CIF)
Crystallographic file for $[Fe_2L_3'']$[PF_6]$_4$ (CIF)

AUTHOR INFORMATION

Corresponding Authors

Michael J. Hannon − *School of Chemistry and Physical Sciences for Health Centre, University of Birmingham, Edgbaston, Birmingham B15 2TT, United Kingdom;* orcid.org/0000-0002-5797-6747; Email: m.j.hannon@bham.ac.uk

David Bardelang − *Aix Marseille Univ, CNRS, ICR, Marseille 13013, France;* orcid.org/0000-0002-0318-5958; Email: david.bardelang@univ-amu.fr

Simin Liu − *The State Key Laboratory of Refractories and Metallurgy, School of Chemistry and Chemical Engineering, Wuhan University of Science and Technology, Wuhan 430081, P. R. China;* orcid.org/0000-0002-8696-4833; Email: liusimin@wust.edu.cn

Authors

Catherine A. J. Hooper − *School of Chemistry, University of Birmingham, Edgbaston, Birmingham B15 2TT, United Kingdom*

Lucia Cardo − *School of Chemistry, University of Birmingham, Edgbaston, Birmingham B15 2TT, United Kingdom*

James S. Craig − *Physical Sciences for Health Centre, University of Birmingham, Edgbaston, Birmingham B15 2TT, United Kingdom*

Lazaros Melidis − *Physical Sciences for Health Centre, University of Birmingham, Edgbaston, Birmingham B15 2TT, United Kingdom*
Aditya Garai − *School of Chemistry, University of Birmingham, Edgbaston, Birmingham B15 2TT, United Kingdom*
Ross T. Egan − *School of Chemistry, University of Birmingham, Edgbaston, Birmingham B15 2TT, United Kingdom*
Viktoriia Sadovnikova − *School of Chemistry, University of Birmingham, Edgbaston, Birmingham B15 2TT, United Kingdom*
Florian Burkert − *School of Chemistry, University of Birmingham, Edgbaston, Birmingham B15 2TT, United Kingdom*
Louise Male − *School of Chemistry, University of Birmingham, Edgbaston, Birmingham B15 2TT, United Kingdom;* orcid.org/0000-0002-8295-2528
Nikolas J. Hodges − *School of Biosciences, University of Birmingham, Edgbaston, Birmingham B15 2TT, United Kingdom*
Douglas F. Browning − *School of Biosciences, University of Birmingham, Edgbaston, Birmingham B15 2TT, United Kingdom*
Roselyne Rosas − *Aix Marseille Univ, CNRS, Centrale Marseille, FSCM, Spectropole, Marseille 13007, France*
Fengbo Liu − *The State Key Laboratory of Refractories and Metallurgy, School of Chemistry and Chemical Engineering, Wuhan University of Science and Technology, Wuhan 430081, P. R. China*
Fillipe V. Rocha − *Department of Chemistry, Federal University of São Carlos, São Carlos 13565-905, Brazil*
Mauro A. Lima − *Department of Chemistry, Federal University of São Carlos, São Carlos 13565-905, Brazil*

Complete contact information is available at: https://pubs.acs.org/10.1021/jacs.0c07750

Author Contributions

⬢These authors contributed equally to this work.

Notes

The authors declare no competing financial interest.

■ ACKNOWLEDGMENTS

This work was funded by the EPSRC Physical Sciences for Health Centre (EP/L016346/1), BBSRC MIBTP (BB/M01116X/1), the EU DNAREC Marie Curie Training Site (MEST-CT-2005-020842), an EU Marie Curie Fellowship (H2020-MSCA-IF-2018-844145), FAPESP (2019/11242-1), National Natural Science Foundation of China (21871216), and the University of Birmingham. Simulations used the Bluebear and Castles HPC facility (U. Birmingham).[77] F.B. was supported by a student exchange from LMU Munich. We thank the Centre for Chemical and Materials Analysis (U. Birmingham), the EPSRC UK National Crystallography Service at the University of Southampton for the collection of the crystallographic data,[78] Dr. Mirela Pascu (U. Birmingham) for some initial experiments (on L′) and Dr. Tim Barendt, Prof. Zoe Pikramenou (both U. Birmingham), Prof Alexandre Martinez (Ecole Centrale de Marseille), and Prof Benoît Colasson (U. Paris Descartes) for helpful discussions.

■ REFERENCES

(1) Stoddart, J. F. Mechanically Interlocked Molecules (MIMs)—Molecular Shuttles, Switches, and Machines (Nobel Lecture). *Angew. Chem., Int. Ed.* **2017**, *56*, 11094−125.
(2) Sauvage, J.-P. From Chemical Topology to Molecular Machines (Nobel Lecture). *Angew. Chem., Int. Ed.* **2017**, *56*, 11080−93.
(3) Zhang, L.; Marcos, V.; Leigh, D. A. Molecular machines with bio-inspired mechanisms. *Proc. Natl. Acad. Sci. U. S. A.* **2018**, *115*, 9397−9404.
(4) Woltering, S.; Gawel, P.; Christensen, K. E.; Thompson, A.L.; Anderson, H.L. Photochemical Unmasking of Polyyne Rotaxanes. *J. Am. Chem. Soc.* **2020**, *142*, 13523−13532.
(5) Danon, J.J.; Leigh, D.A.; McGonigal, P.R.; Ward, J.W.; Wu, J. Triply Threaded [4]Rotaxanes. *J. Am. Chem. Soc.* **2016**, *138*, 12643−12647.
(6) Lewis, J. E. M.; Beer, P.D.; Loeb, S.J.; Goldup, S.M. Metal ions in the synthesis of interlocked molecules and materials. *Chem. Soc. Rev.* **2017**, *46*, 2577−2591.
(7) Ambrogio, M.W.; Thomas, C.R.; Zhao, Y.-L.; Zink, J.I.; Stoddart, J.F. Mechanized Silica Nanoparticles: A New Frontier in Theranostic Nanomedicine. *Acc. Chem. Res.* **2011**, *44*, 903−913.
(8) Pairault, N.; Barat, R.; Tranoy-Opalinski, I.; Renoux, B.; Thomas, M.; Papot, S. Rotaxane-based architectures for biological applications. *C. R. Chim.* **2016**, *19*, 103−112.
(9) Ayme, J. F.; Lehn, J. M. From Coordination Chemistry to Adaptive Chemistry. *Adv. Inorg. Chem.* **2018**, *71*, 3−78.
(10) Albrecht, M.; Chen, X.; Van Craen, D. From Hierarchical Helicates to Functional Supramolecular Devices. *Chem. - Eur. J.* **2019**, *25*, 4265−73.
(11) Cardo, L.; Hannon, M. J. Non-covalent Metallo-Drugs: Using Shape to Target DNA and RNA Junctions and other Nucleic Acid Structures. In *Metals in Life Sciences* Sigel, R., Sigel, H., Sigel, A., Eds.; De Gruyter: Berlin, 2018; Vol. *18*, pp 303−324.
(12) Pöthig, A.; Casini, A. Recent Developments of Supramolecular Metal-based Structures for Applications in Cancer Therapy and Imaging. *Theranostics* **2019**, *9*, 3150−3169.
(13) Allison, S.J.; Cooke, D.; Davidson, F.S.; Elliott, P. I. P.; Faulkner, R.A.; Griffiths, H.B. S.; Harper, O.J.; Hussain, O.; Owen-Lynch, P.J.; Phillips, R.M.; Rice, C.R.; Shepherd, S.L.; Wheelhouse, R.T. Ruthenium-Containing Linear Helicates and Mesocates with Tuneable p53-Selective Cytotoxicity in Colorectal Cancer Cells. *Angew. Chem., Int. Ed.* **2018**, *57*, 9799−9804.
(14) Li, X.; Wu, J.; Wang, L.; He, C.; Chen, L.; Jiao, Y.; Duan, C. Mitochondrial-DNA-Targeted IrIII-Containing Metallohelices with Tunable Photodynamic Therapy Efficacy in Cancer Cells. *Angew. Chem., Int. Ed.* **2020**, *59*, 6420−6427.
(15) Kumar, S.V.; Lo, W. K. C.; Brooks, H. J. L.; Crowley, J.D. Synthesis, structure, stability and antimicrobial activity of a ruthenium(II) helicate derived from a bis-bidentate "click" pyridyl-1,2,3-triazole ligand. *Inorg. Chim. Acta* **2015**, *425*, 1−6.
(16) Domarco, O.; Lotsch, D.; Schreiber, J.; Dinhof, C.; Van Schoonhoven, S.; Garcia, M. D.; Peinador, C.; Keppler, B. K.; Berger, W.; Terenzi, A. Self-assembled Pt2L2 boxes strongly bind G-quadruplex DNA and influence gene expression in cancer cells. *Dalton Trans.* **2017**, *46*, 329−332.
(17) Eskandari, A.; Kundu, A.; Ghosh, S.; Suntharalingam, K. A Triangular Platinum(II) Multinuclear Complex with Cytotoxicity Towards Breast Cancer Stem Cells. *Angew. Chem., Int. Ed.* **2019**, *58*, 12059−12064.
(18) Hrabina, O.; Malina, J.; Kostrhunova, H.; Novohradsky, V.; Pracharova, J.; Rogers, N.; Simpson, D.H.; Scott, P.; Brabec, V. Optically Pure Metallohelices That Accumulate in Cell Nuclei, Condense/Aggregate DNA, and Inhibit Activities of DNA Processing Enzymes. *Inorg. Chem.* **2020**, *59*, 3304−3311.
(19) Adamski, A.; Fik, M. A.; Kubicki, M.; Hnatejko, Z.; Gurda, D.; Fedoruk-Wyszomirska, A.; Wyszko, E.; Kruszka, D.; Dutkiewicz, Z.; Patroniak, V. Full characterization and cytotoxic activity of new silver(I) and copper(I) helicates with quaterpyridine. *New J. Chem.* **2016**, *40*, 7943−7957.

(20) Qin, H.; Zhao, C.; Sun, Y.; Ren, J.; Qu, X. Metallo-supramolecular Complexes Enantioselectively Eradicate Cancer Stem Cells in Vivo. *J. Am. Chem. Soc.* **2017**, *139*, 16201−16209.
(21) Hannon, M. J.; Moreno, V.; Prieto, M. J.; Moldrheim, E.; Sletten, E.; Meistermann, I.; Isaac, C. J.; Sanders, K. J.; Rodger, A. Intramolecular DNA coiling mediated by a metallo supramolecular cylinder. *Angew. Chem., Int. Ed.* **2001**, *40*, 879−884.
(22) Meistermann, I.; Moreno, V.; Prieto, M. J.; Moldrheim, E.; Sletten, E.; Khalid, S.; Rodger, P. M.; Peberdy, J. C.; Isaac, C. J.; Rodger, A.; Hannon, M. J. Intramolecular DNA coiling mediated by metallo-supramolecular cylinders: differential binding of P and M helical enantiomers. *Proc. Natl. Acad. Sci. U. S. A.* **2002**, *99*, 5069−5074.
(23) Ducani, C.; Leczkowska, A.; Hodges, N. J.; Hannon, M. J. Noncovalent DNA-Binding Metallo-Supramolecular Cylinders Prevent DNA Transactions in vitro. *Angew. Chem., Int. Ed.* **2010**, *49*, 8942−8945.
(24) Oleksi, A.; Blanco, A.G.; Boer, R.; Usón, I.; Aymami, J.; Rodger, A.; Hannon, M.J.; Coll, M. Molecular recognition of a three-way DNA junction by a metallo-supramolecular helicate. *Angew. Chem., Int. Ed.* **2006**, *45*, 1227−1231.
(25) Phongtongpasuk, S.; Paulus, S.; Schnabl, J.; Sigel, R. K. O.; Spingler, B.; Hannon, M. J.; Freisinger, E. Binding of a Designed Anti-Cancer Drug to the Central Cavity of an RNA Three-Way Junction. *Angew. Chem., Int. Ed.* **2013**, *52*, 11513−11516.
(26) Boer, D. R.; Kerckhoffs, J. M. C. A.; Parajo, Y.; Pascu, M.; Uson, I.; Lincoln, P.; Hannon, M. J.; Coll, M. Towards functionalizable DNA frames: Self assembly of two-component 3D DNA arrays through induction of DNA three-way junction branch points by supramolecular cylinders. *Angew. Chem., Int. Ed.* **2010**, *49*, 2336−2339.
(27) Cerasino, L.; Hannon, M. J.; Sletten, E. DNA Three-Way Junction with a Dinuclear Iron(II) Supramolecular Helicate at the Center: A NMR structural Study. *Inorg. Chem.* **2007**, *46*, 6245−6251.
(28) Malina, J.; Hannon, M. J.; Brabec, V. Recognition of DNA Three-Way Junctions by Metallosupramolecular Cylinders: Gel Electrophoresis Studies. *Chem. - Eur. J.* **2007**, *13*, 3871−3877.
(29) Martinez, C.R.; Iverson, B.L. Rethinking the term "pi-stacking. *Chem. Sci.* **2012**, *3*, 2191−2201.
(30) Duskova, K.; Lamarche, J.; Amor, S.; Caron, C.; Queyriaux, N.; Gaschard, M.; Penouilh, M.-J.; de Robillard, G.; Delmas, D.; Devillers, C.H.; Granzhan, A.; Teulade-Fichou, M.-P.; Chavarot-Kerlidou, M.; Therrien, B.; Britton, S.; Monchaud, D. Identification of three-way DNA junction ligands through screening of chemical libraries and validation by complementary in vitro assays. *J. Med. Chem.* **2019**, *62*, 4456−66.
(31) Duskova, K.; Lejault, P.; Benchimol, É.; Guillot, R.; Britton, S.; Granzhan, A.; Monchaud, D. DNA junction ligands trigger DNA damage and are synthetic lethal with DNA repair inhibitors in cancer cells. *J. Am. Chem. Soc.* **2020**, *142*, 424−35.
(32) van Rixel, V. H. S.; Busemann, A.; Wissingh, M. F.; Hopkins, S. L.; Siewert, B.; van de Griend, C.; Siegler, M. A.; Marzo, T.; Papi, F.; Ferraroni, M.; Gratteri, P.; Bazzicalupi, C.; Messori, L.; Bonnet, S. Induction of a Four-Way Junction Structure in the DNA Palindromic Hexanucleotide 5'-d(CGTACG)-3' by a Mononuclear Platinum Complex. *Angew. Chem., Int. Ed.* **2019**, *58*, 9378−9382.
(33) Chien, C.-M.; Wu, P.-C.; Satange, R.; Chang, C.-C.; Lai, Z.-L.; Hagler, L.D.; Zimmerman, S.C.; Hou, M.-H. Structural Basis for Targeting T:T Mismatch with Triaminotriazine- Acridine Conjugate Induces a U-Shaped Head-to-Head Four-Way Junction in CTG Repeat DNA. *J. Am. Chem. Soc.* **2020**, *142*, 11165−11172.
(34) Brogden, A. L.; Hopcroft, N. H.; Searcey, M.; Cardin, C. J. Ligand bridging of the DNA Holliday junction: molecular recognition of a stacked-X four-way junction by a small molecule. *Angew. Chem., Int. Ed.* **2007**, *46*, 3850−3854.
(35) Zhu, J.; Haynes, C.J. E.; Kieffer, M.; Greenfield, J.L.; Greenhalgh, R.D.; Nitschke, J.R.; Keyser, U.F. $Fe^{II}_4L_4$ Tetrahedron Binds to Nonpaired DNA Bases. *J. Am. Chem. Soc.* **2019**, *141*, 11358−11362.
(36) Hotze, A. C. G.; Hodges, N. J.; Hayden, R. E.; Sanchez-Cano, C.; Paines, C.; Male, N.; Tse, M.-K.; Bunce, C. M.; Chipman, J. K.; Hannon, M. J. A supramolecular triple-stranded iron cylinder with unprecedented DNA binding action is a potent cytostatic and apoptotic agent without exhibiting genotoxicity. *Chem. Biol.* **2008**, *15*, 1258−1267.
(37) Cardo, L.; Nawroth, I.; Cail, P. J.; McKeating, J. A.; Hannon, M. J. Metallo supramolecular cylinders inhibit HIV-1 TAR-TAT complex formation and viral replication in cellulo. *Sci. Rep.* **2018**, *8*, 13342.
(38) Pope, A. J.; Bruce, C.; Kysela, B.; Hannon, M. J. Issues surrounding standard cytotoxicity testing for assessing activity of non-covalent DNA-binding metallo-drugs. *Dalton Trans.* **2010**, *39*, 2772−2774.
(39) Cardo, L.; Sadovnikova, V.; Phongtongpasuk, S.; Hodges, N. J.; Hannon, M. J. Arginine conjugates of metallo-supramolecular cylinders prescribe helicity and enhance DNA junction binding and cellular activity. *Chem. Commun.* **2011**, *47*, 6575−6577.
(40) Pérez, E. M. Putting Rings around Carbon Nanotubes. *Chem. - Eur. J.* **2017**, *23*, 12681−12689.
(41) Barrejón, M.; Mateo-Alonso, A.; Prato, M. Carbon Nanostructures in Rotaxane Architectures. *Eur. J. Org. Chem.* **2019**, *2019*, 3371−3383.
(42) Xu, Y.; Kaur, R.; Wang, B.; Minameyer, M.B.; Gsañger, S.; Meyer, B.; Drewello, T.; Guldi, D.M.; von Delius, M. Concave-Convex π-π Template Approach Enables the Synthesis of [10]-Cycloparaphenylene-Fullerene [2]Rotaxanes. *J. Am. Chem. Soc.* **2018**, *140*, 13413−13420.
(43) Ackermann, D.; Schmidt, T.L.; Hannam, J.S.; Purohit, C.S.; Heckel, A.; Famulok, M. A double-stranded DNA rotaxane. *Nat. Nanotechnol.* **2010**, *5*, 436−442.
(44) Moretto, A.; Menegazzo, I.; Crisma, M.; Shotton, E.J.; Nowell, H.; Mammi, S.; Toniolo, C. A Rigid Helical Peptide Axle for a [2]Rotaxane Molecular Machine. *Angew. Chem., Int. Ed.* **2009**, *48*, 8986−8989.
(45) Yang, X. R.; Liu, F. B.; Zhao, Z. Y.; Liang, F.; Zhang, H. J.; Liu, S. M. Cucurbit[10]uril-based chemistry. *Chin. Chem. Lett.* **2018**, *29*, 1560−1566.
(46) Liu, S. M.; Zavalij, P. Y.; Isaacs, L. Cucurbit[10]uril. *J. Am. Chem. Soc.* **2005**, *127*, 16798−16799.
(47) Shetty, D. P.; Khedkar, J. K.; Park, K. M.; Kim, K. Can we beat the biotin-avidin pair?: cucurbit[7]uril-based ultrahigh affinity host-guest complexes and their applications. *Chem. Soc. Rev.* **2015**, *44*, 8747−8761.
(48) Isaacs, L. Stimuli Responsive Systems Constructed Using Cucurbit[n]uril-Type Molecular Containers. *Acc. Chem. Res.* **2014**, *47*, 2052−2062.
(49) Barrow, S. J.; Kasera, S.; Rowland, M. J.; del Barrio, J.; Scherman, O. A. Cucurbituril-Based Molecular Recognition. *Chem. Rev.* **2015**, *115*, 12320−12326.
(50) Assaf, K. I.; Nau, W. M. Cucurbiturils: from synthesis to high-affinity binding and catalysis. *Chem. Soc. Rev.* **2015**, *44*, 394−418.
(51) Murray, J.; Kim, K.; Ogoshi, T.; Yao, W.; Gibb, B. C. The aqueous supramolecular chemistry of cucurbit[n]urils, pillar[n]arenes and deep-cavity cavitands. *Chem. Soc. Rev.* **2017**, *46*, 2479−2496.
(52) Cheng, Q.; Yin, H.; Rosas, R.; Gigmes, D.; Ouari, O.; Wang, R.; Kermagoret, A.; Bardelang, D. A pH-driven ring translocation switch against cancer cells. *Chem. Commun.* **2018**, *54*, 13825−8.
(53) Villarroel-Lecourt, G.; Carrasco-Carvajal, J.; Andrade-Villalobos, F.; Solis-Egana, F.; Merino-San Martin, I.; Robinson-Duggon, J.; Fuentealba, D. Encapsulation of Chemotherapeutic Drug Melphalan in Cucurbit[7]uril: Effects on Its Alkylating Activity, Hydrolysis, and Cytotoxicity. *ACS Omega* **2018**, *3*, 8337−8343.
(54) Gong, W. J.; Yang, X. R.; Zavalij, P. Y.; Isaacs, L.; Zhao, Z. Y.; Liu, S. M. From Packed "Sandwich" to "Russian Doll": Assembly by Charge-Transfer Interactions in Cucurbit[10]uril. *Chem. - Eur. J.* **2016**, *22*, 17612−17618.

https://dx.doi.org/10.1021/jacs.0c07750
J. Am. Chem. Soc. 2020, 142, 20651−20660

(55) Kuang, S.; Hu, Z.; Zhang, H.; Zhang, X.; Liang, F.; Zhao, Z.; Liu, S.M. Enhancement of metal-metal interactions inside a large-cavity synthetic host in water. *Chem. Commun.* **2018**, *54*, 2169−2171.
(56) Liu, S. M.; Shukla, A. D.; Gadde, S.; Wagner, B. D.; Kaifer, A. E.; Isaacs, L. Ternary complexes comprising cucurbit[10]uril, porphyrins, and guests. *Angew. Chem., Int. Ed.* **2008**, *47*, 2657−2660.
(57) Yu, Y.; Li, Y. W.; Wang, X. Q.; Nian, H.; Wang, L.; Li, J.; Zhao, Y. X.; Yang, X. R.; Liu, S. M.; Cao, L. P. Cucurbit[10]uril-Based [2]Rotaxane: Preparation and Supramolecular Assembly-Induced Fluorescence Enhancement. *J. Org. Chem.* **2017**, *82*, 5590−6.
(58) Masson, E.; Raeisi, M.; Kotturi, K. Kinetics Inside, Outside and Through Cucurbiturils. *Isr. J. Chem.* **2018**, *58*, 413−434.
(59) Wang, S.R.; Wang, J.Q.; Xu, G.H.; Wei, L.; Fu, B.S.; Wu, L.Y.; Song, Y.Y.; Yang, X.R.; Li, C.; Liu, S.M.; Zhou, X. The Cucurbit[7]-Uril-Based Supramolecular Chemistry for Reversible B/Z-DNA Transition. *Adv. Sci.* **2018**, *5*, 1800231.
(60) Wu, H.; Chen, H.; Tang, B.; Kang, Y.; Xu, J.-F.; Zhang, X. Host-Guest Interactions between Oxaliplatin and Cucurbit[7]uril/Cucurbit[7]uril Derivatives under Pseudo-Physiological Conditions. *Langmuir* **2020**, *36*, 1235−4.
(61) Chen, Y.; Huang, Z.; Zhao, H.; Xu, J.F.; Sun, Z.; Zhang, X. Supramolecular Chemotherapy: Cooperative Enhancement of Anti-tumor Activity by Combining Controlled Release of Oxaliplatin and Consuming of Spermine by Cucurbit[7]uril. *ACS Appl. Mater. Interfaces* **2017**, *9*, 8602−8.
(62) Cao, L.; Hettiarachchi, G.; Briken, V.; Isaacs, L. Cucurbit[7]uril Containers for Targeted Delivery of Oxaliplatin to Cancer Cells. *Angew. Chem., Int. Ed.* **2013**, *52*, 12033−12037.
(63) Jin Jeon, Y.; Kim, S.-Y.; Ho Ko, Y.; Sakamoto, S.; Yamaguchi, K.; Kim, K. Novel Molecular Drug Carrier: Encapsulation of Oxaliplatin in Cucurbit[7]uril and Its Effects on Stability and Reactivity of the Drug. *Org. Biomol. Chem.* **2005**, *3*, 2122.
(64) Wheate, N. J. Improving Platinum(II)-Based Anticancer Drug Delivery Using Cucurbit[n]urils. *J. Inorg. Biochem.* **2008**, *102*, 2060−6.
(65) Bali, M.S.; Buck, D.P.; Coe, A.J.; Day, A.I.; Collins, J.G. Cucurbituril binding of trans-$[\{PtCl(NH_3)_2\}_2((\text{-}NH_2(CH_2)_8NH_2)]^{2+}$ and the effect on the reaction with cysteine. *Dalton Trans.* **2006**, *45*, 5337−5344.
(66) Li, F.; Gorle, A. K.; Ranson, M.; Vine, K. L.; Kinobe, R.; Feterl, M.; Warner, J. M.; Keene, F. R.; Collins, J. G.; Day, A. I. Probing the Pharmacokinetics of Cucurbit[7, 8 and 10]uril: And a Dinuclear Ruthenium Antimicrobial Complex Encapsulated in Cucurbit[10]uril. *Org. Biomol. Chem.* **2017**, *15*, 4172−9.
(67) Sun, B.; Musgrave, I. F.; Day, A. I.; Heimann, K.; Keene, F. R.; Collins, J. G. Eukaryotic Cell Toxicity and HSA Binding of $[Ru(Me4phen)(Bb7)]^{2+}$ and the Effect of Encapsulation in Cucurbit[10]uril. *Front. Chem.* **2018**, *6*, 00595.
(68) Harris, D. H. *Quantitative Chemical Analysis*, 9th ed.; WH Freeman & Co.: New York, 2015.
(69) McGonigal, P.R. Multiply threaded rotaxanes. *Supramol. Chem.* **2018**, *30*, 782−794.
(70) Danon, J.J.; Leigh, D.A.; McGonigal, P.R.; Ward, J.W.; Wu, J. Triply Threaded [4]Rotaxanes. *J. Am. Chem. Soc.* **2016**, *138*, 12643−12647.
(71) Cheng, H.M.; Leigh, D.A.; Maffei, F.; McGonigal, P.R.; Slawin, A. M. Z.; Wu, J. En Route to a Molecular Sheaf: Active Metal Template Synthesis of a [3]Rotaxane with Two Axles Threaded through One Ring. *J. Am. Chem. Soc.* **2011**, *133*, 12298−12303.
(72) Wang, X.; Smithrud, D.B. Pt-rotaxanes as cytotoxic agents. *Bioorg. Med. Chem. Lett.* **2011**, *21*, 6880−3.
(73) Sojka, M.; Fojtu, M.; Fialova, J.; Masarik, M.; Necas, M.; Marek, R. Locked and Loaded: Ruthenium(II)-Capped Cucurbit[n]-uril-Based Rotaxanes with Antimetastatic Properties. *Inorg. Chem.* **2019**, *58*, 10861−70.
(74) Barat, R.; Legigan, T.; Tranoy-Opalinski, I.; Renoux, B.; Péraudeau, E.; Clarhaut, J.; Poinot, P.; Fernandes, A. E.; Aucagne, V.; Leigh, D. A.; Papot, S. A mechanically interlocked molecular system programmed for the delivery of an anticancer drug. *Chem. Sci.* **2015**, *6*, 2608−2613.
(75) Fernandes, A.; Viterisi, A.; Coutrot, F.; Potok, S.; Leigh, D.A.; Aucagne, V.; Papot, S. Rotaxane-Based Propeptides: Protection and Enzymatic Release of a Bioactive Pentapeptide. *Angew. Chem., Int. Ed.* **2009**, *48*, 6443−6447.
(76) Fernandes, A.; Viterisi, A.; Aucagne, V.; Leigh, D. A.; Papot, S. Second generation specific-enzyme-activated rotaxane propeptides. *Chem. Commun.* **2012**, *48*, 2083−2085.
(77) Thompson, S. J.; Thompson, S. E. M.; Cazier, J.-B. CaStLeS (Compute and Storage for the Life Sciences): a collection of compute and storage resources for supporting research at the University of Birmingham; *Birmingham Environment for Academic Research*; **2019** DOI: 10.5281/zenodo.3250616.
(78) Coles, S. J.; Gale, P. A. Changing and Challenging Times for Service Crystallography. *Chem. Sci.* **2012**, *3*, 683−9.

https://dx.doi.org/10.1021/jacs.0c07750
J. Am. Chem. Soc. 2020, 142, 20651−20660